



Origin of iron and aluminium in large particles (>53 μm) in the Crozet region, Southern Ocean

Hélène Planquette^{a,b,*}, Gary R. Fones^c, Peter J. Statham^a, Paul J. Morris^a

^a National Oceanography Centre, University of Southampton, European Way, Southampton, SO14 3ZH, United Kingdom

^b Institute of Marine and Coastal Sciences, Rutgers University, 71 Dudley Road, New Brunswick, NJ 08901-8525, USA

^c School of Earth and Environmental Sciences, University of Portsmouth, Burnaby building, Burnaby Road, Portsmouth, PO1 3QL, United Kingdom

ARTICLE INFO

Article history:

Received 28 April 2008

Received in revised form 23 March 2009

Accepted 1 June 2009

Available online 11 June 2009

Regular index terms:

Southern Ocean
Crozet Islands

Keywords:

Suspended particulate matter
Iron
Aluminium
HNLC
CROZEX

ABSTRACT

Natural iron fertilization processes are occurring around the Crozet Islands (46°26'S–52°18'E), thus relieving the water masses from the normally encountered High Nutrients Low Chlorophyll (HNLC) conditions of the Southern Ocean. During austral summers 2004/2005 and 2005/2006, iron and aluminium concentrations were investigated in large particles (>53 μm) collected from just below the mixed layer at stations under the influence of island inputs, and also in adjacent HNLC waters. These large particles are anticipated to sink out of the mixed layer, and to reflect the net effects of input and cycling of these elements in the overlying mixed layer. Labile and refractory fractions were determined by a two-stage leaching technique. Data showed that water masses downstream of the islands were enriched in total iron and aluminium (0.25–2.68 nmol L^{-1} and 0.34–3.28 nmol L^{-1} respectively), relative to the southern HNLC control sites (0.15–0.29 nmol L^{-1} for Fe and 0.12–0.29 nmol L^{-1} for Al), with only a small fraction (typically <1%) being acid leachable in both environments. Particulate iron predominantly derived from the island system represents a significant fraction of the total water column iron inventory and may complement dissolved Fe inputs that help support the high summer productivity around the Crozet islands.

Published by Elsevier B.V.

1. Introduction

One of the major objectives of marine geochemistry is to understand the global distribution, sources and sinks and reactions of key elements involved in biogeochemical cycles. The importance of iron to primary production in High Nutrient Low Chlorophyll (HNLC) waters such as the Southern Ocean is now well established (e.g. De Baar et al., 1995) and the Crozet Islands in the Southern Ocean provide an “in situ” laboratory (Pollard et al., 2007a) where natural iron fertilization processes can be studied. Recent results indicate that the waters located north of the plateau are affected by a horizontal advective input of dissolved iron originating from the islands and surrounding Plateau in addition to vertical and atmospheric supply (Charette et al., 2007; Planquette et al., 2007).

In surface waters, active fixation of dissolved elements such as iron during phytoplankton growth converts many chemical elements into particulate matter, and the fraction not recycled in the mixed layer may then be transported as large aggregates or particles to the deep ocean (Kuss and Kremling, 1999). Chemical species that are passively adsorbed, complexed or co-precipitated in particulate matter will also

follow similar routes out of the euphotic zone. The fate of iron associated with particles sinking out of the upper water column is unclear as it may be recycled to dissolved forms in the upper thermocline and then be returned to the mixed layer by convective processes, or it may escape the thermocline and be transferred to the deep ocean and remineralized in this environment. This particulate material leaving the mixed layer will also represent the net product of inputs and cycling processes in the overlying water column. The form and fate of this particulate iron therefore has important implications for primary production in the Southern Ocean.

However, few studies have considered Fe in large particles (>53 μm) (Frew et al., 2006; Lam et al., 2006) despite the fact that the pool of iron in the upper water column is dominated by the particulate fraction (De Baar and de Jong, 2001). Furthermore, the environmental reactivity of particulate iron or any element cannot be assessed exclusively by its total concentration. Numerous carrier phases and types of associations are possible between trace elements and suspended particulate matter (SPM). SPM may consist of biological and mineral phases, which will each contain different coordination sites to bind metals (Stumm, 1992). Identification and quantification of elements present in different phases or fractions within a sample will therefore provide more information (Tovar-Sanchez et al., 2003). The origin of the particulate iron pool is either lithogenic or biogenic (Morel and Price, 2003), but operational

* Corresponding author. Institute of Marine and Coastal Sciences, Rutgers University, 71 Dudley Road, New Brunswick, NJ 08901-8525, USA. Tel.: +1 732 932 6555x257.

E-mail address: heleneplanquette@marine.rutgers.edu (H. Planquette).

separations by filtration and/or various chemical leaching schemes can only partly make the distinction. Aluminium concentrations in particles are also important as they can be used to provide a clear indication of what fraction of the iron present is associated with aluminosilicate phases. The Al content has conventionally been used to estimate the continental contribution to marine sediments (Saito et al., 1992), and can also help to identify a lithogenic source in the present work.

However, it is very useful with regard to the role of Fe in biology, to distinguish by physical/chemical separation a “potentially biologically active” phase from a “refractory” phase (Landing and Bruland, 1987). This way, it is possible to examine the consequences of natural iron fertilization on the composition of these large particles.

In the present paper, measurements of particulate iron and aluminium in the acid leachable and refractory phases of large particles from the base of the mixed layer around the Crozet Islands that have been shown to be a natural source of iron (Planquette et al., 2007) are presented. The objectives of this study are to provide new insights into the origin and properties of particulate Fe in this environment.

2. Materials and methods

Samples were taken during the three cruises of the CROZEX (Pollard et al., 2007a; Wolff, 2007) project on RRS *Discovery* in the austral summer of 2004/05 (2 cruises) and 2005/06 (1 cruise) in the waters surrounding the Crozet Islands. A variety of sites were sampled, including locations under the influence of the islands and control sites, located south of the islands (Fig. 1).

2.1. Sampling methods

Several sampling devices are available for the collection of sinking particles: fixed sediment traps (moored or tethered), neutrally buoyant sediment traps and in situ pumps. Fixed sediment traps allow a quantitative collection of particles on long time scales but their main disadvantage is that this collection can be biased by hydrodynamic features in the sampling zone, swimmers attacks and resolubilization effects (Gardner, 2000). Therefore, a new generation of Lagrangian free floating traps sediment traps has emerged (e.g. Valdes and Price,

2000), these new devices being able to capture falling particles without letting it swept past by currents. This type of trap has been used extensively during VERTIGO (Buesseler et al., 2008) and during CROZEX (Salter et al., 2007; Lampitt et al., 2008). However, because of evident contamination of some samples with paint flakes in PELAGRA traps found after recovery (recent versions of PELAGRA have overcome this problem) the accurate determination of trace metals was not possible. Instead, particles were collected from >1000 L of seawater using in situ pump systems (Stand Alone Pump Systems; SAPS, Challenger Oceanic) deployed on a plastic coated hydrographic line. This allowed the clean filtration of large volumes of seawater without using too much wire time (typically 3.5 h per deployment) and the collection of sufficient material for a representative sample (Weinstein and Moran, 2004). The filter holder and head were made of polypropylene (PP) and PVC, and butyl O-rings sealed the assembly. The filter was a 53 µm nylon mesh monofilament screen (300-mm diameter) chosen because particles above this size are considered to be the major sinking size fraction, and therefore responsible for exporting carbon and other elements from surface waters (Bishop et al., 1985). Each filter was acid washed in 10% HCl solution, rinsed, dried, weighed and stored in double resealable plastic bags. Before each deployment, the PP filter holder was soaked in 10% Micro[®] (detergent solution, VWR) for 2 to 3 days, depending on the frequency of the stations, and rinsed with fresh Milli-Q deionised water just before deployment. The pump head was covered with a plastic bag to exclude any particles from the ship environment until the last minute of the deployment.

The parameters used for deciding each deployment depth were water temperature, fluorescence and transmission. These measurements were performed during a CTD deployment just before deploying the SAPS. SAPS were then placed at a depth that would collect the sinking particles that were falling out of the biologically productive surface layers of the water column and were therefore deployed about 10 m below the base of the thermal mixed layer. Pumps were typically set to run for 1.5 h, except at two stations where the biomass had a high concentration and a 60-minute pump time was chosen (D285, Station M3.2; D300, Crozet 1) to preserve the filters from any clogging or damage. Volumes ranged between 1001 L (M5, Table 2) and 2434 L (Crozet 1). The sampling details for the three cruises are given in Table 2

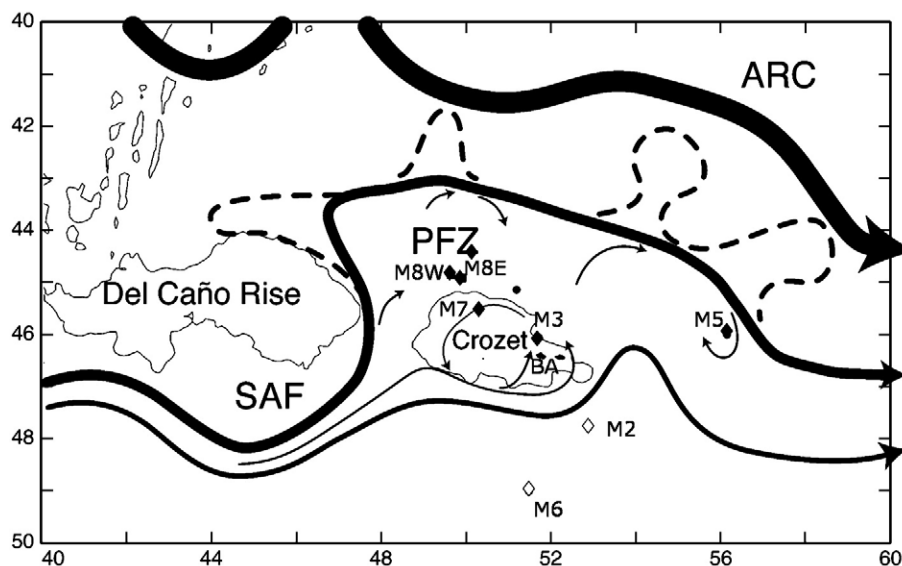


Fig. 1. Schematic of the circulation around Crozet. The thick black line marks the Agulhas Return Current (ARC), the bold solid line is the SubAntarctic Front (SAF), with dashed lines between them marking transient, propagating eddies. Thin arrows represent the very weak circulation in the Polar Frontal Zone (PFZ) between the SAF and Crozet. They show anticyclonic circulation round Crozet, Ekman flow past the islands, meanders breaking off the SAF into the region and re-entrainment of eddies into the SAF. Eastward flow south of Crozet is also shown. For spatial reference, the 2000 m contour is the light solid line. From Pollard et al., 2007. Northern stations (♦) under the influence of islands are distinguished from the Southern stations (◊) which can be considered as the control sites.

Table 1

Quality control results of replicate analyses of metals in standard reference materials.

	Blank	BIR-1	JA-2	JB-2	MAG-1	No. 9 NIES	SGR-1	TORT-2
Al	0.00031 ± 0.00012 (n = 5)	<i>8.12 ± 0.27*</i> 10.24 ± 0.35 (n = 4) 118%	<i>8.15*</i> 9.35 ± 0.29 (n = 3) 111%	<i>7.74*</i> 7.45 ± 0.75 (n = 3) 100%	<i>16.64 ± 0.3*</i> 18.45 ± 0.11 (n = 3) 108%	<i>215</i> 213 ± 3.92 (n = 3) 100%	<i>6.52 ± 0.21*</i> 6.58 ± 0.14 (n = 3) 100%	– 5.18 ± 0.23 (n = 4) 105 ± 13
Fe	0.0011 ± 0.00075 (n = 5)	<i>7.87B ± 0.16*</i> 8.47 ± 2.6 (n = 4) 100%	<i>4.34*</i> 4.25 ± 0.66 (n = 3) 100%	<i>9.96*</i> 10.35 ± 0.37 (n = 3) 100%	<i>6.8 ± 0.6*</i> 8.47 ± 0.84 (n = 3) 103%	<i>187 ± 6</i> 180.5 ± 9.2 (n = 3) 100%	<i>3.03 ± 0.14*</i> 2.70 ± 0.12 (n = 3) 98%	103.7 ± 6.05 (n = 4) 100%

Certified concentrations are in italics. Concentrations obtained in this study are in bold. % value is recovery. All concentrations are expressed in ppm except for *: wt.%. MAG-1: Marine mud, United States Geological Survey (USGS). SGR-1: Oil Shale of the Green River Formation, USGS. BIR-1: Icelandic basalt, Reykjavik dolerites, 12 km east of Reykjavik, Iceland. JB-2: Basalt from Oshima volcano erupted in 1950–51, Oshima, Tokyo, Geological Survey of Japan. JA-2: Andesite, Goshikidai sanukitoid, 14 Ma, Sakaide, Kagawa Prefecture, GSJ. No. 9 NIES: Sargasso Seaweed, National Institute for Environmental Studies (NIES), Japan. TORT-2: Hepatopancreas of lobster, NRC Canada: no values where reported for Al.

Immediately after recovery and separation of the head from the SAPS body, excess water in the housing was drawn off under vacuum in a laminar flow hood. Various “swimmers” (i.e. copepods mainly) were removed manually with cleaned tweezers and placed in vials, and then the filter was immediately put in a freezer at $-20\text{ }^{\circ}\text{C}$ to avoid any physical or chemical changes until analysis back in the laboratory. At the same time, except during D300, samples for the determination of particulate organic carbon (POC), and particulate organic nitrogen (PON) were taken (Morris et al., 2007) using another SAPS deployed simultaneously at the same depth. Sub-samples were taken for POC/PON from the same filter for the trace metal analysis during D300 only and placed into pre-weighed and pre-combusted silver cups. These transfer steps and the relatively small amount (1–2 mg) of particles analyzed may have had an impact on the representative nature of the POC/PON values used for the interpretation of the D300 results. However, this factor appears small given the similar range of POC/PON ratios found relative to those measured during D285 and D286.

2.2. Analysis of trace metals, POC/PON and BSI

2.2.1. Two step metal analysis procedure

Unfortunately, there is no universal dissolution procedure valid for every type of sample, but a choice has been made in this study to distinguish: a) the “labile” fraction, which comprises those metals weakly sorbed onto organic matter, associated with amorphous oxyhydroxides and carbonate minerals, and b) the more refractory fraction, such as aluminosilicates and crystalline Fe oxyhydroxides.

The procedure extracts firstly the labile fraction by a 25% acetic acid leach (e.g., Landing and Bruland, 1987; Fitzwater et al., 2003; Lewis and Landing, 1992; Löscher, 1999; Wells et al., 2000), with the residue after this extraction being completely digested with aqua regia and hydrofluoric acid (HF). The particles were rinsed from the nylon filter prior to analysis to a) remove any associated salt b) separate the particles from the mesh for which high blank values have been reported (Weinstein and Moran, 2004), and which is not possible to fully digest and c) ease of handling as manipulating the nylon material is difficult. Therefore the particles from the nylon filter were washed off with sub-boiling distilled water (SBDW) and collected onto pre-weighed 0.4 μm polycarbonate filters (Cyclopore). The nylon mesh and the filters were then freeze dried for 12 h and weighed using an electro-microbalance (Mettler AE240) for mass determination of the SPM. Recoveries of particles on the filters were on average 80%.

2.2.1.1. 1st leach: 25% acetic acid (HAc). The dried Cyclopore filters were placed in Teflon vials with 5 to 12 mL of 25% (v/v) quartz-distilled HAc (Q-HAc, sub-boiled distilled water) and soaked for 2 h at room temperature according to the protocol of Wells et al. (2000). They were then transferred with the solution into 10 mL polypropylene centrifuge tubes and centrifuged (2500 rpm for 45 min). The overlying solution was transferred to clean Teflon pots (30 mL screw cap) and taken to dryness on a hotplate (110 $^{\circ}\text{C}$). The residues were brought into solution by addition of 4 mL of 2% Q-HNO₃, this solution was being kept for analysis by ICP-MS. The refractory residue was

rinsed out of the tube with SBDW directly into a Teflon pot (15 mL screw cap) then dried on a hot plate at 140 $^{\circ}\text{C}$, ready for the second acid attack.

2.2.1.2. 2nd leach: total digestion. The refractory fraction was brought into solution by a total digestion using aqua regia and hydrofluoric acid (HF) (Eggiman and Betzer, 1976), which completely releases the trace elements including the aluminosilicate phases. Because of the possibility of trace element loss due to volatilization at higher temperatures, all processing steps were done in closed Teflon pots (15 mL screw cap, Savillex).

The reagents (HCl, HNO₃, HF) used in the dissolution procedures were all high purity, or double-sub-boiled distilled acid and all operations were performed in a clean room. The first stage of the digestion was made with 2.4 mL of concentrated aqua regia for 24 h at 140 $^{\circ}\text{C}$, the solution taken to dryness and followed by a hydrofluoric acid (HF, 0.4 mL)/nitric (HNO₃, 0.8 mL) dissolution at 140 $^{\circ}\text{C}$ for 24 h of any opal or silicates which may have been present. With a few samples, any residual organic matter was further digested by a heating evaporation cycle with more HNO₃ and HF (samples from Stations BA and M6.2).

Finally, a 24 h reduction step with 2 mL of 6 M HCl was done to drive off the fluorides. Following complete dissolution, the solution was evaporated to dryness and redissolved in 2% HNO₃ and kept in clean 15 mL low density polyethylene (LDPE) bottles (Nalgene) until analysis. Blank solutions (n = 6) were treated in the same manner as the sample and provide a total chemistry blank solution. A very small amount of acid migration through the threads during heating was noted occasionally but blank runs indicated no significant contamination from the pots (Table 1).

2.2.2. ICP-MS analysis

All analyses of the solutions obtained after the two acid attacks described previously were performed using an Agilent 7500ce ICP-MS (Inductively Coupled Plasma-Mass Spectrometer) and an integrated auto-sampler (I-AS). The 7500ce uses an octopole reaction system to eliminate any spectral interferences. The reaction system can be run in two modes; reaction mode using hydrogen gas which was used for the analysis of Fe⁵⁶ and collision mode using helium gas which was used for the analysis of Al²⁷. The use of the octopole reaction system eliminates any polyatomic spectral interferences and the need for interference corrections.

A dilution factor of 10–4600 (depending on iron concentration) was applied to each sample and certified reference material. Whilst a wide range of elements were analysed, Fe and Al data are presented and discussed in this study. The data processing procedure used the Agilent software Chemstation and included linear drift correction, blank subtraction, calibration, and a dilution correction. For this work, mixed standards were prepared in the range of 0.1 to 200 $\mu\text{g L}^{-1}$ in 2% nitric solution. If one sample was found to fall significantly outside of this range, it was diluted by a greater factor and run again. An internal standard of 20 $\mu\text{g L}^{-1}$ Rh and Bi (stock solution of 400 $\mu\text{g L}^{-1}$ Rh and Bi with twenty fold online dilution) was used to determine any

variation in the intensity of their signal. This correction is made automatically by the software.

The accuracy and precision of the total trace element analyses in SPM were determined using Certified International Standard Reference Materials (JA-2; JB-2; MAG-1; SGR-1; BIR-1, TORT-2 and No.9 (NIES) that were processed in the same manner and at the same time as the samples. The values are reported in Table 1 with the blank values ($n=5$). All data are blank corrected. The recoveries from the CRMs ranged between 98 and 108% of the recommended concentrations for both trace metals. The concentrations of metals in the analytical blank was ca. $0.00031 \mu\text{g g}^{-1}$ for Al and $0.0011 \mu\text{g g}^{-1}$ for Fe, and these values are between two and five orders of magnitude lower than the concentrations found in the samples.

2.2.3. POC/PON analysis

Sub-samples (D300 samples only) of the collected particles and samples (D285 and D286) were placed in combusted and pre-weighed silver cups for final analysis. Samples were initially fumigated with concentrated sulphuric acid in a vacuum desiccator for 48 h to destroy any inorganic carbonates present (modified from Verado et al., 1990). Samples were then dried at 60°C for a further 48 h before analysis with a POC/PON Carlo-Erba NA-1500 elemental analyzer, using standardization with acetanilide. The relative standard deviation of analytical replicates was $<13\%$ ($n=3$) for both POC and PON. Procedural blanks for C and N demonstrated that sample contamination was negligible ($<1\%$).

2.2.4. BSi analysis

A full description can be found in Salter et al. (2007). In brief, aliquots were taken from the filter and dried at 60°C for 24 h. Then, they were dissolved using 0.2 M sodium hydroxide for 3 h at 110°C . The solution was then centrifuged (3000 rpm, 15 min) and the sediment residue was rinsed with ultra-pure water and dried overnight (60°C). A second sodium hydroxide digestion was performed to make sure that all particulate silica was removed.

The absorbance of the silicomolybdate complex (Strickland and Parsons, 1968) was read at 812 nm with a Hitachi U-2000 spectrophotometer. Biogenic opal was calculated assuming 10% water content of silicon dioxide, a value typically reported for marine diatoms (Mortlock and Froelich, 1989).

3. Results and discussion

A brief overview of the circulation and the characteristics of the water masses will be first presented. Then, the distribution of particulate phases on a mass per volume basis as well as the Fe to Al ratios will be discussed in order to help identify the origin of the iron.

3.1. Hydrographic setting, primary production and dissolved iron concentrations

A full description of the main characteristics of the circulation in the area can be found in Pollard et al. (2007b) and are summarized in Fig. 1. In overview, the path of the Sub Antarctic Front (SAF) is initially deflected northwards by the Del Caño rise before reflecting eastwards and then moving slightly southwards and to the east. This path, together with the plateau to the south creates a mostly enclosed area to the north of the islands within the Polar Front Zone (PFZ) that has a long water residence time in the range of 60 to 100 days (Venables et al., 2007). Therefore, the bloom is constrained to the west and north by the SAF, and is likely to be under the influence of a weak and northerly surface flow that passes over and past the Crozet Plateau and Islands. Thus south of Crozet is “upstream”, north of Crozet is “downstream” of the islands.

In the austral summer 2004/2005 (Fig. 2), the northerly region was characterised initially by high productivity and chlorophyll ($0.5\text{--}1.1 \text{ g C m}^{-2} \text{ d}^{-1}$ and $5 \mu\text{g Chlorophyll L}^{-1}$ respectively) and a *Phaeocystis* dominated phytoplankton assemblage from mid November to early December (Seeyave et al., 2007). Declining community biomass to the north of the plateau subsequently resulted in a microflagellate-dominated community and a mixture of diatoms and *Phaeocystis* dominated the secondary bloom that developed in mid January. To the south of the plateau, biomass and productivity were generally low throughout the study period, with a small peak in chlorophyll observed in the satellite data in December, and a community composed of microflagellates, cyanobacteria and fewer giant diatoms (Poulton et al., 2007). For the austral summer 2005/2006 (Fig. 2), the bloom in October was self contained within the PFZ, with chlorophyll *a* reaching concentrations greater than $3 \mu\text{g L}^{-1}$. A filament of this bloom extended southwards, following the northern boundary of the SAF. In November, chlorophyll *a* concentrations were still high but the bloom was limited to the area immediately surrounding the plateau. In January, no secondary bloom could be noticed and the chlorophyll levels dropped down to $1 \mu\text{g L}^{-1}$ with a thin filament located north of the plateau that was deflected to the east.

Dissolved iron (D_{Fe} , $<0.2 \mu\text{m}$) distributions were also investigated during D285 and D286 and detailed results can be found in Planquette et al. (2007). To summarize, D_{Fe} concentrations varied between 0.086 and 0.25 nM in the top 100 m, both to the North and to the South of the Plateau, and no clear distinction between these zones was evident. However, enrichment of dissolved iron (up to 2.48 nM) at close proximity to the islands indicates that the plateau and the associated sediments are a source of dissolved iron. This source appeared to be the largest component of the iron inputs to the waters north of the Crozet Islands when compared to atmospheric and vertical mixing inputs. Waters to the north of the islands appeared to be affected by this input of coastal and shelf origin and dissolved iron concentrations decreased as a function of distance from the islands with a gradient of 0.07 nM km^{-1} at the time of sampling (Charette et al., 2007).

3.2. Distribution and POC/N content of SPM immediately below the mixed layer

Concentrations of $>53 \mu\text{m}$ SPM (Table 2) varied from $8 \mu\text{g L}^{-1}$ (Station M3.4) up to $90.3 \mu\text{g L}^{-1}$ (Station M8W). The majority (nearly 60%) of the concentrations found over the three cruises were lower than $30 \mu\text{g L}^{-1}$. On only two occasions did concentrations reach $90 \mu\text{g L}^{-1}$. At M3, this high concentration was measured 13 days after the maximum peak in chlorophyll *a* of $2.5 \mu\text{g L}^{-1}$, due to a community dominated by diatoms (Poulton et al., 2007), which is also reflected in the relatively high BSi concentration. The second occasion occurred at M8W and was associated with high productivity (Seeyave et al., 2007; Read et al., 2007) with *Phaeocystis antarctica* dominating the community (Poulton et al., 2007). The southern sites (M2 and M6 occupations hereafter) that are not under the influence of the islands have slightly higher concentrations of SPM, on average $38 \mu\text{g L}^{-1}$ whereas the northern sites (M3, M5, M7, M8E, M8W occupations hereafter) have a mean concentration of suspended particulate matter of $32 \mu\text{g L}^{-1}$ (Table 2). Therefore, it is impossible to distinguish the northern sites from the southern sites in terms of SPM concentrations. These concentrations are within the range of published data in oligotrophic areas (Table 3), and are the first to be reported in the Southern Ocean for large particles.

There is a clear relationship between the SPM and POC concentrations at all sites, with a very good correlation between POC and SPM concentrations in both regions (South: $r^2=0.97$, $n=5$; North: $r^2=0.81$, $n=17$) as shown in Fig. 3, indicating that the samples were mainly biogenic in origin, with the fraction of POC being between 5% (Station Crozet 1, D300) and 31% (Station M5, D286) of

the total mass of SPM collected. Moreover, on average the sum of POC, PON and BSi (Biogenic Silica) accounts for 70% of the mass of SPM collected (Table 2). POC concentrations ranged from 0.04 $\mu\text{mol L}^{-1}$ (Crozet 1, D300) to 0.89 $\mu\text{mol L}^{-1}$ (M8W). The lowest POC concentration and therefore biomass was found at the station closest to Île de la Possession, supporting the hypothesis that phytoplankton growth must have been inhibited by the high turbidity regimes and subsequent low light availability (Planquette et al., 2007).

3.3. Particulate iron and aluminium concentrations

All results are given in Table 2 and shown in Fig. 4. Total particulate (>53 μm) metal concentrations (P-Me) are the sum of the acetic acid leachable (HAc-Me) and refractory (Ref-Me) measured concentrations. Results are discussed in relation to the three main Crozet regimes: downstream of the islands (i.e. northern sites), upstream of the islands (i.e. southern sites) and at close proximity to the islands.

3.3.1. Southern sites (M2, M6)

These sites have low acid leachable aluminium and iron concentrations (HAc-Al and HAc-Fe respectively): the lowest concentrations were measured at station M2.2 (0.08 pmol L^{-1} for HAc-Fe and 0.26 pmol L^{-1} for HAc-Al). The lowest concentrations of total PFe (0.29 and 0.15 nmol L^{-1}) are found at stations M6.1 and M2.1 respectively at the beginning of the survey, and southern sites had average PFe and PAI concentrations of 0.20 and 0.21 nmol L^{-1} respectively, which are significantly less than the northern sites demonstrating that this zone does not have significant inputs from the nearby islands. These PAI values are very similar to the open Southern Ocean values reported by Dehairs et al. (1992) for the Scotia–Weddell confluence where particulate aluminium (>0.45 μm) ranged between 1 and 9 nmol L^{-1} , and to the off-shelf typical HNLC sites sampled near the Kerguelen Islands during the recent KEOPS cruise (Jacquet et al., 2008) where particulate aluminium (>0.4 μm) ranged between 1 and 17 nmol L^{-1} (Table 3).

3.3.2. Northern sites (M3, M5, M7, M8E, M8W)

These stations are under the influence of the islands and had higher average total iron and aluminium concentrations (average PFe and PAI concentrations of 0.95 and 1.19 nmol L^{-1} respectively) than the Southern sites. The variability of these concentrations is demonstrated for example by Station M3, where PFe concentrations varied from 1.74 nmol L^{-1} down to 0.25 nmol L^{-1} . On average, concentrations of total particulate iron are greater in the north than the south, by at least a factor of 3. It is more difficult to establish a difference between the fertilized sites and non-fertilized sites by looking at only the acid leachable concentrations that vary between 0.57 (M2.1) and 8.84 (M3.2) pmol L^{-1} for HAc-Al and between 0.08 (M2.2) and 11.7 (M3.2) pmol L^{-1} for HAc-Fe.

3.3.3. Crozet area

Maximum concentrations of HAc-Fe were obtained at Baie Américaine (BA), reaching 22.2 pmol L^{-1} and at another station very close (14 km) to Île de la Possession, where the HAc-Fe concentration was 17.6 pmol L^{-1} . These high values, 10 times greater than the average measured elsewhere support the hypothesis that the islands are a source of potentially bioavailable iron. Particles were enriched by a factor of almost 100 compared to the particles sampled at other sites. Station Crozet 1 also had a quite high total values at 70 m, in comparison with the concentrations observed near the bottom (340 m depth), where Fe concentrations are close to the average of the concentrations in the north. This corresponds as well to a low labile fraction noticed in the previous section for this sample. The BA Station had the highest total concentrations of Al (25.5 nmol L^{-1}) and Fe (13.2 nmol L^{-1}), and particles collected at this station also have the greatest total concentrations of Fe on a mass per mass

Table 2
Acid leachable (HAc), refractory (Ref) and total (P) Fe and Al, and SPM, POC, PON, Biogenic Si concentrations during D285 (light grey shading), D286 (dark grey shading) and D300.

Station #	Date Dd/mm/yy	Latitude (°S)	Longitude (°E)	Water column depth (m)	Deployment depth (m)	Volume filtered (L)	SPM >53 μm $\mu\text{g L}^{-1}$	POC $\mu\text{mol L}^{-1}$	PON $\mu\text{mol L}^{-1}$	BSi $\mu\text{mol L}^{-1}$	HAc-Al pmol L^{-1}	Ref-Al nmol L^{-1}	PAI nmol L^{-1}	HAc-Fe pmol L^{-1}	Ref-Fe nmol L^{-1}	PFe nmol L^{-1}
M3.1	13/11/2004	46.0577	51.7806	2398	225	1933	89.9	0.86	0.133	1.05	4.6	3.23	3.23	1.58	1.74	1.74
M3.2	18/11/2004	46.0260	51.8105	2353	155	1502	12.8	0.19	0.035	0.12	8.84	2.47	2.48	11.7	1.37	1.38
M2.1	19/11/2004	47.7955	52.8554	3857	150	2017	30.3	0.3	0.053	0.12	0.57	0.2	0.20	0.4	0.15	0.15
M6.1	21/11/2004	49.0056	51.5005	4227	200	2053	33.5	0.26	0.050	0.09	1.47	0.27	0.27	0.96	0.29	0.29
M3.3	25/11/2004	46.0701	51.7715	2331	200	1990	21.7	0.33	0.056	0.19	1.38	0.46	0.46	0.46	0.25	0.25
M7	27/11/2004	45.4989	49.0017	2749	150	1940	45.9	0.45	0.090	0.23	0.66	0.68	0.68	0.41	0.38	0.38
M8E	29/11/2004	44.9535	49.9410	2750	200	1972	34.4	0.34	0.056	0.08	4.98	1.61	1.61	2.68	0.8	0.80
M8W	01/12/2004	44.8724	49.6471	2816	150	1842	90.3	0.89	0.134	0.41	1.54	0.67	0.67	0.35	1.41	1.41
M3.4	22/12/2004	46.0683	51.7782	2363	180	1945	8.23	0.17	0.028	0.05	1.02	0.33	0.33	0.82	0.4	0.40
M5	27/12/2004	45.9974	56.1521	4271	125	1001	15.8	0.41	0.034	0.11	1.03	0.58	0.58	0.38	0.38	0.38
M3.5	31/12/2004	46.0432	51.7779	2358	100	1909	17.6	0.23	0.034	0.23	0.28	1.93	1.93	0.36	1.5	1.50
M6.2	03/01/2005	48.9990	51.5380	4214	120	1878	67.8	0.55	0.084	0.56	0.38	0.19	0.19	2.18	0.22	0.22
M2.2	06/01/2005	47.8003	52.8484	3858	160	1653	51	0.47	0.074	0.31	0.26	0.28	0.28	0.08	0.27	0.27
M3.7	10/01/2005	46.0323	51.8704	2320	80	1493	8.43	0.16	0.027	0.16	1.47	0.47	0.47	3.52	0.38	0.38
M3.8	12/01/2005	46.0409	51.9606	2514	80	2031	10.9	0.26	0.043	0.19	0.14	0.84	0.84	1.78	0.66	0.66
D300 M5.1	08/12/2005	46.0038	56.2668	4261	140	2169	43.4	0.4	0.043	-	2.32	1.1	1.10	0.27	2.68	2.68
D300 M5.2	24/12/2005	45.9402	56.4248	4122	100	2278	25.1	0.53	-	-	0.52	1.08	1.08	0.12	0.42	0.42
D300 M6.1	04/01/2006	49.1072	51.2093	4192	110	2359	16.5	0.16	-	-	0.62	0.11	0.11	0.3	0.16	0.16
Crozet 1	06/01/2006	46.4992	51.9163	359	70	2434	8.92	0.04	-	-	12.9	2.51	2.52	17.6	1.25	1.27
Crozet 2	06/01/2006	46.4992	51.9163	359	340	2313	15.7	0.33	0.05	-	4.11	1.49	1.49	1.96	0.8	0.80
BA	06/01/2006	46.3807	51.8293	69	30	1647	26.6	0.34	0.05	-	32.5	25.5	25.5	22.2	13.2	13.2

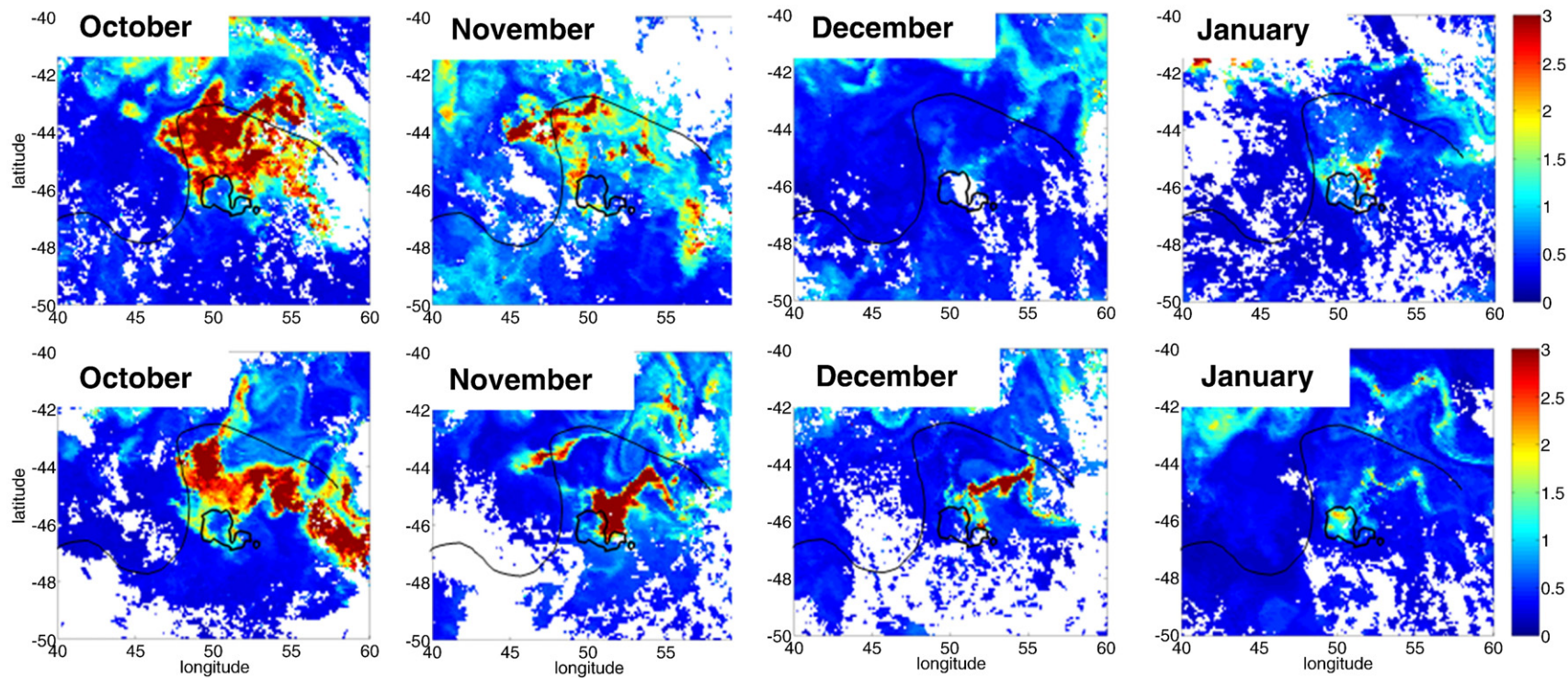


Fig. 2. SeaWiFS/MODIS images around Crozet of Austral summers 2004/2005 (D285 and D286, top) and 2005/2006 (D300 m, bottom) centred on the study area presented in Fig. 1. The Crozet Plateau is represented by a light black solid line as well as a branch of the Antarctic Circumpolar Current, the Sub Antarctic Front. Satellite images were provided by Hugh Venables (NOCS/BAS). Concentrations are expressed in $\mu\text{g L}^{-1}$.

Table 3

Iron and aluminium concentrations in suspended particulate matter from surface and shelf waters in diverse regions of the world ocean.

Location	Particle size (μm)	Depth (m)	SPM (mg L^{-1})	Total Al (nmol L^{-1})	Total Fe (nmol L^{-1})	HAc-Al (nmol L^{-1})	HAc-Fe (nmol L^{-1})	Reference
Southern Ocean: Pacific sector, 47°S–61°S	0.2	15			0.9			Tovar-Sanchez et al., 2003
Pacific: 120–160°W; 20°S 40°N	0.3	15–4900	0.007–0.39	0.89–260	0.1–61.5	0.01–4.91	0.01–10.8	Landing and Bruland, 1987
California coastal waters	0.4	surface	0.24–4.31	1.0–2323	0.2–359	0.1–24	0.02–23.1	Fitzwater et al., 2003
Antarctic coastal water Ross Sea	0.4	2–380	0.15–4.31		1.1–58.5			Grotti et al., 2001
Polar front zone: 42–55°S 141.5–143°E	0.4	20–200		1.2–100				Cardinal et al., 2001
Polar Front zone: 59–68°S–170°W	0.4	0–500		0.05–0.47	0.02–0.24	0.01–0.17	0.006–0.13	Coale et al., 2005
Kerguelen Islands 50.62°S, 78.00 °E	0.4	0–800		0.0–1838				Jacquet et al., 2008
Southern Ocean: 46.24°S–178°E	20	25		1.10–2.40	0.20–0.33			Frew et al., 2006
Sargasso Sea	1.0–53	0–100		1.2–6.7	0.32			Sherrell and Boyle, 1992
Labrador Sea	53	0–250		0.1–1.5	0.1–1.2			Weinstein and Moran, 2004
Gulf of Maine	53	0–300	0.05–0.6	0.1–50	0.1–32			Weinstein and Moran, 2004
Equatorial Atlantic Ocean					1.9–3.8			Bishop and Fleisher, 1987; Bishop et al., 1977; Cullen and Sherrell, 1999
California coast: 36.36°N 122°W	53	0–80		60–850				Lam et al., 2006
Subartic Pacific	53	12–900			0.005–2.476			Lam et al., 2006
Southern Ocean: 55°S 172°W	53				0.08–4			Lam et al., 2006
Southern Ocean: Crozet Islands	53	30–340	0.008–0.090	0.11–25.5	0.15–13.2	0.0002–0.03	0.0008–0.022	This study

Note that sampling depth and filter pore size vary between studies.

basis (27.7 mg g^{-1}). This is in line with the results of the 1st leach and again supports the view that the islands are a likely source of particulate as well as dissolved iron (Planquette et al., 2007). Moreover, these sites are associated with low chlorophyll *a* and low biomass (Venables et al., 2007), and have the highest HAc/Total iron molar ratios, suggesting that these large particles of lithogenic origin could possibly be available to the phytoplankton as they are advected to the north.

The variations in acid leachable Fe concentrations (from 0.08 pmol L^{-1} at M2.2 up to 22.2 pmol L^{-1} at BA) reveal the importance of biological processes during SPM ($>53 \mu\text{m}$) formation. Lowest concentrations were found in the iron-limited sites to the south. There is a clear net difference between the northern and southern sites in terms of particle composition, with the particles found in the north being enriched in Fe.

Overall, the spatial distribution of particulate ($>53 \mu\text{m}$) Al concentrations follows the same pattern as for PFe. At the Southern sites HAc-Al range from 0.26 to 1.47 pmol L^{-1} (M2.2 and M6.1 respectively) whilst HAc-Al concentrations range from 0.14 to

8.84 pmol L^{-1} (M3.8 and M3.2 respectively) in the North. The maximum concentrations are obtained in Baie Américaine, reaching 32.5 pmol L^{-1} . The total aluminium concentrations follow the same general distribution of total Fe; southern sites are less enriched in aluminium with concentrations ranging from 0.11 to 0.28 nmol L^{-1} (D300 M6.1 and M2.2 respectively) whilst downstream sites have much higher PAI concentrations, up to 3.23 nmol L^{-1} at M3.1. The maximum PAI concentration was at Baie Américaine, with 25.5 nmol L^{-1} .

Studies conducted on particulate trace metals in the Southern Ocean are scarce and mainly focused on the small (>0.2 – $0.4 \mu\text{m}$) particulate metal fraction (e.g. Coale et al., 2005). However, a recent study by Lam et al. (2006) reported some results for the large fraction ($>53 \mu\text{m}$) in the Southern Ocean. Data from all recent studies are reported in Table 3, including information from those conducted in the Pacific (Landing and Bruland, 1987), Sargasso Sea (Sherrell and Boyle, 1992), Gulf of Maine and Labrador sea (Weinstein and Moran, 2004), in the Atlantic Ocean (Bishop et al., 1977; Bishop and Fleisher, 1987) and off the coast of California (Fitzwater et al., 2003).

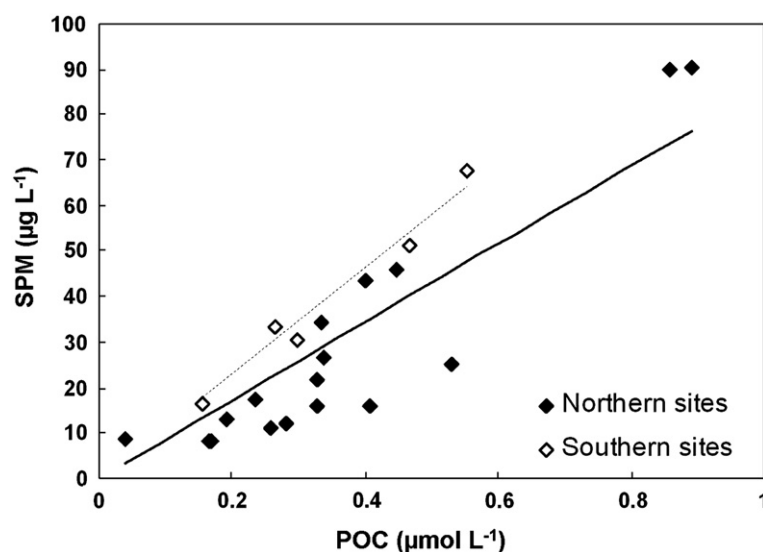


Fig. 3. POC versus SPM concentrations during D285, D286 and D300. A distinction is made between the Northern sites (◆, Stations M3, M5, M7, M8E, M8W, M10) and Southern sites (◇, M2 and M6).

Concentrations of both trace elements considered in this study are within the range of published data in the Southern Ocean (e.g. Lam et al., 2006, Frew et al., 2006). The highest values of total Fe obtained near Crozet are similar to those reported by Grotti et al. (2001) in Antarctic coastal waters. The values for Al and Fe found at the BA station are greater than the results published for the open Southern Ocean, confirming a local island source of trace metals (Charette et al., 2007; Planquette et al., 2007). However, these high particulate Al values measured at the BA station are two orders of magnitude less than what was measured above the plateau close to Heard Island during KEOPS (Jacquet et al., 2008).

The high PAI concentrations provide the most convincing evidence of terrestrial input within this zone. Therefore, to estimate the lithogenic fraction of these particles, it is possible to use Al as an elemental proxy (e.g. Goldberg and Arrhenius, 1958; Frew et al., 2006). Aluminium occurs at a high and relatively constant abundance in a variety of rock and basalt types. In the following section, spatial distribution of particulate aluminium will be described,

in order to identify the various inputs of aluminium in the two contrasting sites.

3.4. Evidence for a lithogenic island source of Fe and Al

Enhanced PAI concentrations in the northern sites are argued here to reflect the input from the islands of basalt debris and strong horizontal fluxes. Clear evidence for a lithogenic source of particulate matter to the north of the islands can be found by considering the total particulate molar Fe/Al ratios. Where this ratio is similar to the average Crozet Islands basalt crust ratio of 0.51 (Gunn et al., 1970) a lithogenic source predominates. Higher ratios in suspended particles may be expected because of the scavenging of dissolved iron and other trace elements relative to aluminium on the outer surface of the particles (Murray et al., 1993, 2000; Van Cappellen and Qiu, 1997a,b). Molar particulate Fe/Al ratios are reported for the northern and southern regions as well as in Baie Américaine in Table 4 and are shown in Fig. 5.

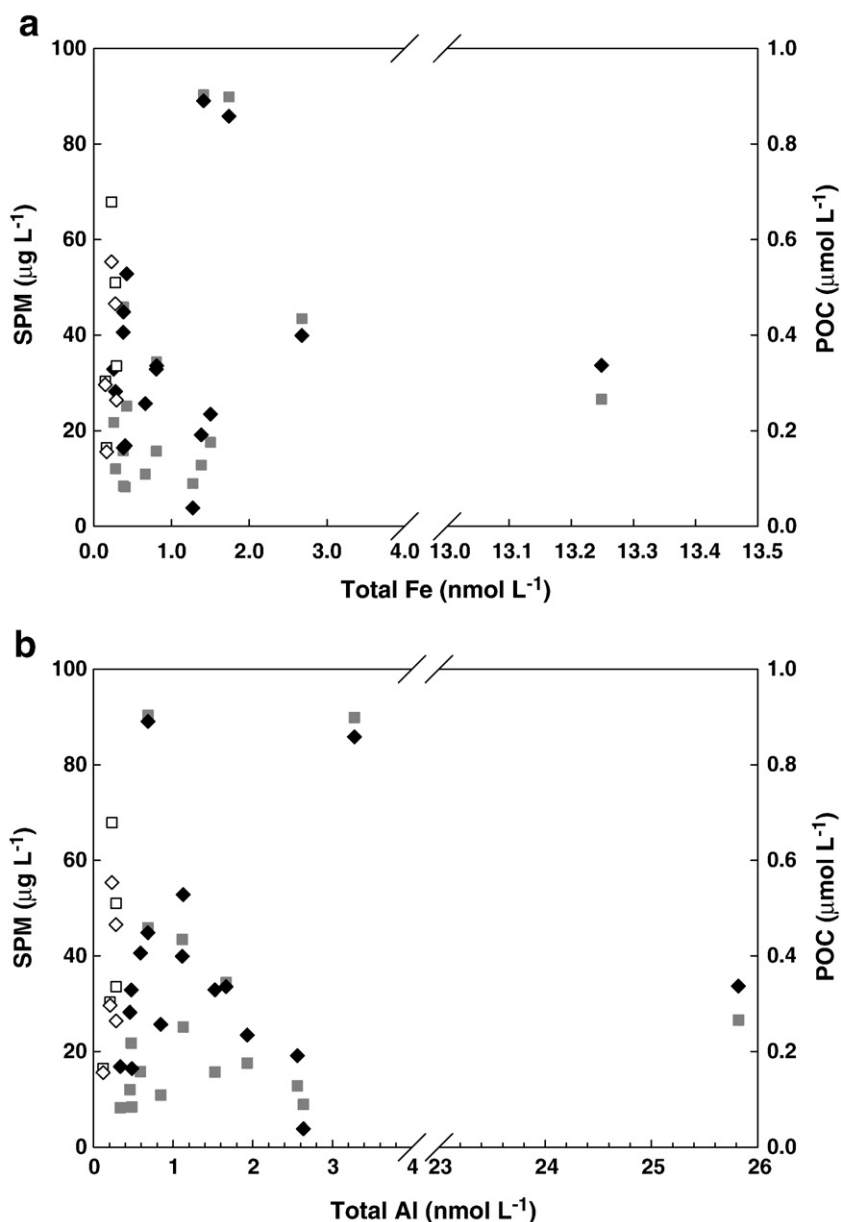


Fig. 4. Total Fe (4a) and Al (4b) versus POC (diamonds) and SPM (squares) concentrations. Data points for southern sites are open symbols with no fill.

Table 4

Elemental molar ratios calculated during D285, D286 and D300.

Station #	PFe/PAI molar ratio	Lithogenic Fe* (nmol L ⁻¹)	Biogenic Fe* (nmol L ⁻¹)	% Litho Fe	PFe/C molar ratio ($\mu\text{mol}:\text{mol}$)	HAC-Fe/C molar ratio ($\mu\text{mol}:\text{mol}$)	FS
M3.1	0.54	1.65	0.09	95	2025	1.84	6.47
M3.2	0.56	1.26	0.12	91	7272	61.6	5.43
M2.1	0.75	0.10	0.05	68	501	1.33	5.66
M6.1	1.07	0.14	0.15	48	1119	3.69	5.2
M3.3	0.54	0.24	0.02	94	759	1.39	5.89
M7	0.56	0.35	0.03	91	845	0.91	5.06
M8E	0.50	0.82	-0.02	103	2361	7.88	6.07
M8W	2.10	0.34	1.07	24	1585	0.39	6.64
M3.4	1.21	0.17	0.23	42	2358	4.82	6.07
M5	0.65	0.30	0.08	78	928	0.93	
M3.5	0.78	0.98	0.52	66	6523	1.57	
M6.2	1.17	0.10	0.13	44	404	3.96	7.43
M2.2	0.96	0.14	0.13	53	575	0.17	
M3.7	0.81	0.24	0.14	63	2397	22.0	
M3.8	0.79	0.43	0.23	65	2545	6.85	
D300 M5.1	0.39	0.55	-0.13	131	793	0.23	
D300 M6.1	1.45	0.06	0.10	35	1002	1.88	
Cr ozet 1 75m	0.50	1.29	-0.02	102	31690	440	
Cro zet 2 340m	0.54	0.76	0.04	95	2430	5.94	6.6
BA	0.52	13.0	0.20	98	38889	65.3	6.8

*Lithogenic and biogenic Fe concentrations are calculated by assuming a basalt Fe/Al ratio of 0.51 (Gunn et al., 1970); see text for details.

Overall, whilst the total particulate Fe/Al ratios were variable throughout the sampling period, on average, the southern sites have a higher ratio than the northern sites. At Baie Américaine stations the Fe/Al ratios approached the average basalt crust ratio of 0.51 (Gunn et al., 1970), as would be anticipated close to the volcanic island system of the Crozet Archipelago (Fig. 5).

The Fe/Al molar ratios in the northern area (Table 4) are up to 2.10 (M8W) and can be explained by a high diatom production transferring particulate matter out of the mixed layer which is reflected here by the POC concentration ($0.89 \mu\text{mol L}^{-1}$). Also, the transfer of Fe in lithogenic material from the islands to the North may stimulate primary production, which can then lead to the removal of lithogenically derived iron from the mixed layer. The concentration of total Fe in the SPM collected at the base of the mixed layer can reflect the efficient removal of particulate Fe with biogenic material and/or that particulate Fe can be a non-negligible source of Fe stimulating natural fertilization processes (Lam et al., 2006). The high Fe/Al ratio observed in the south (M6.1 and M6.2) could reflect an external input of

particulate iron such as an atmospheric source (Planquette et al., 2007), where the Fe/Al ratio varied from 0.35 to 0.88 (Alex Baker, pers. comm.), together with gradual scavenging of iron in waters advected from the west.

If it is assumed that all particulate aluminium derives from lithogenic material (Frew et al., 2006), it is possible to calculate the biogenic iron fraction, which is defined as the difference between the total concentration and the lithogenic concentration. These values are also reported in Table 4. The percent lithogenic component ranged from 24 (M8W) to 131% (M5.1), which is in the same range as found in the study of Frew et al. (2006) (24–122%). Uncertainties in these calculations include the assumption of a constant Fe/Al molar ratio for lithogenic material within the particles.

These data indicate that a significant fraction of iron is of lithogenic origin, with a maximum in the north (M5.2). The samples taken in the vicinity of Baie Américaine had a high percentage of lithogenic iron (98%, Table 2). On average, the lithogenic particulate iron pool represents 68% of the total particulate iron pool which is in agreement

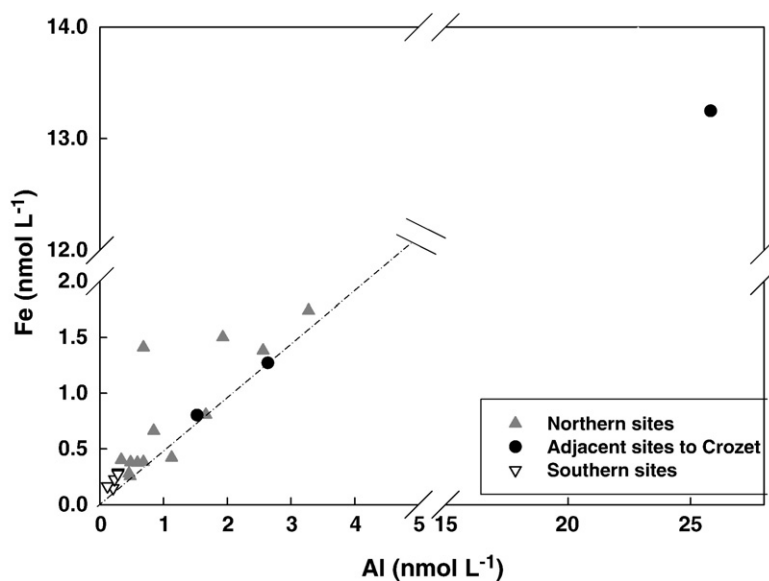


Fig. 5. Fe versus Al concentrations at both sites. The basalt ratio is symbolized by the light grey dashed line. Note that Baie Américaine is not represented on this figure in order to make the other data points clearly visible.

with the data set of Frew et al. (2006), and with the data reported by Strzeppek et al. (2005) where the Fe is mainly lithogenic in particles above 20 μm .

However, the calculated biogenic fraction is one order of magnitude greater than the measured HAC-Fe concentrations. This result suggests that the HAC-Fe fraction may not reflect the sum of all bioavailable iron. The biogenic fraction as defined above will include Fe that may become associated with particles through a variety of processes including adsorption, oxide precipitation, colloid aggregation or agglomeration prior to active or inactive biological uptake. All of these phases will not be available to the acetic acid leach (e.g. some oxides will not be dissolved (Berger et al., 2008)).

3.5. Particulate iron (53 μm), in relation to particulate organic carbon and nitrogen

Elemental ratios (PFe:C and C:N) are given in Table 4 and plotted as a function of latitude in Fig. 6. With the exception of the stations close to the main islands, the C:N ratios are in a similar range to those of Frew et al. (2006). However, most of them are below the usual Redfield C:N ratio of 6.6 as estimated by Hedges et al. (2002) for Southern Ocean suspended particulate matter. This may reflect a high copepod grazing pressure and associated particle production, which occurred predominantly in the iron-limited oceanic stations (typically M2, M6 and M3.2) during the second leg of the first cruise (Fielding et al., 2007). Microzooplankton pressure has not been assessed in this region during the different cruises so this effect will remain unknown.

High Fe:C reflects the significant lithogenic component of Fe at these sites downstream of the islands. During the FeCycle experiment in Southern Ocean HNLC waters, for particles greater than 20 μm , Frew et al. (2006) observed Total PFe:C molar ratios ranging between 167 and 218 $\mu\text{mol}:\text{mol}$, which is at least an order of magnitude smaller than those calculated here. This is consistent with an island system source of Fe being supplied to this region, and also supports the view that particulate carbon could be preferentially recycled relative to Fe (Frew et al., 2006), and/or Fe from other sources (e.g. dissolved forms from the island) is adsorbed onto the particles. Atmospheric inputs of dissolved Fe to the Crozet region were also estimated ($\sim 100 \text{ nmol m}^{-2} \text{ d}^{-1}$; Planquette et al., 2007) and provide a low level input term distributed over the whole study area, but nonetheless they may provide additional iron to fuel any small blooms to the south of the islands.

A labile Fe to C molar ratio can also be calculated, and in the present study ranged from 0.17 to 440 (M2.2 and Crozet 1 respectively).

If the high HAC-Fe/C ratios obtained very close to the Crozet Islands (Crozet 1, Crozet 2, BA) are excluded from this analysis, then the upper bound is 22 obtained at M3.7. Löscher et al. (1997) also reported HAC-Fe:C average ratios of $\sim 5\text{--}10$ ($>0.2 \mu\text{m}$ fraction). These values are lower than those reported here, especially in the area downstream of the islands, which is again consistent with significant amounts of iron coming from an island lithogenic input.

4. Conclusions

A two step leaching technique was applied to large ($>53 \mu\text{m}$) particles at the base of the mixed layer to assess the distribution of labile and refractory Al and Fe around the Crozet Islands in order to test the hypothesis of a lithogenic input of Fe from the island system. The concentration of SPM, Fe and Al as well as the POC export (Morris et al., 2007) was highly variable during the survey, revealing the complexity of processes occurring in this region. The SPM was dominated by biogenic material and the acetic acid leachable fraction of Fe ranged from 0.02% to nearly 1% of the total Fe, typical of large particles in the ocean (Wells et al., 1991), but there was no systematic difference in HAC concentrations between north and south of the islands. In contrast the average total Fe and Al concentrations were higher to the north (downstream) of the islands. The highest concentrations of total Al and Fe were found at close proximity to the islands, and reached concentrations up to 150 times higher than the other sites visited. In combination the data provide compelling evidence of an island source of particulate Fe downstream of the islands that is in addition to the dissolved source already identified (Planquette et al., 2007).

When the “biogenic” fraction of Fe is calculated (Frew et al., 2006), this value is typically greater than the acetic acid leachable fraction. This suggests that at least some of the Fe in particles that is associated with biota is not available to the acetic acid leach (Berger et al., 2008). Both the acetic acid leachable Fe/C and “biogenic” Fe/C are higher downstream of the islands relative to the upstream HNLC zones. This would seem to reflect the enhanced supply of Fe to biota downstream of the islands or a preferential cycling of C relative to Fe. As the acetic leach is unlikely to represent all of the “bioavailable” fraction, there is a need to identify a method for distinguishing the refractory from the bioavailable fractions.

However, the main fraction of total Fe in the particles collected below the mixed layer around Crozet are of lithogenic origin, but only a small fraction of this pool is likely to be bioavailable to organisms.

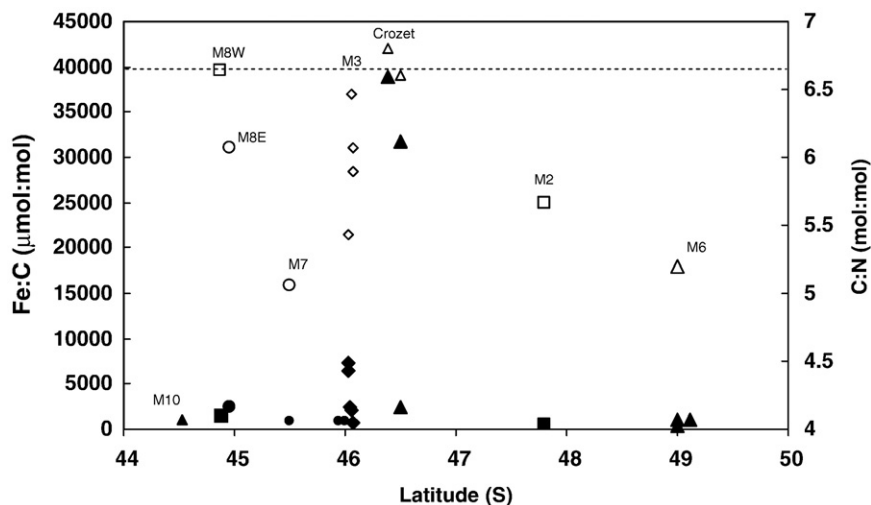


Fig. 6. Elemental molar ratios of particulate material (open C:N; filled Fe:C) during D285, D286, D300. The long dash dot line represents the standard Redfield ratios.

Further investigations will require the study of mechanisms that can deliver bioavailable iron from this important lithogenic pool.

The results presented here (in particular at station M3) support the recent study of Lam et al. (2006) who argue that the transport and availability of particulate iron can affect the productivity of open HNLC regions hundreds of kilometres downstream from the source. It is important to remember that here we only consider large particles at the base of the mixed layer, and it is anticipated that the smaller size fractions within the upper water column will contain from 2 to 10 times higher concentrations of Fe than the >53 µm fraction, (Lam et al., 2006). This fraction of Fe is likely to be more readily accessed by the phytoplankton and could represent up to 70% of the dissolved iron budget (Dehairs et al., 1992). Processes governing the size fractionation within the euphotic zone remains unknown in this study and the particle size spectrum differences between the northern and southern sites will have to be explored in future studies.

Acknowledgments

The authors would like to thank all the scientists and crew on board RRS *Discovery* during cruises D285, D286 and D300, Tina Hayes for her help with the digestion procedures, Hugh Venables for satellite images, Sophie Seeyave for the primary productivity data, Ian Salter for the BSI data and Phoebe Lam for her valuable comments. This work was supported by NERC grant NE/B502844/1.

References

- Berger, C.J.M., Lippiatt, S.M., Lawrence, M.G., Bruland, K.W., 2008. Application of a chemical leach technique for estimating labile particulate aluminum, iron, and manganese in the Columbia River plume and coastal waters off Oregon and Washington. *J. Geophys. Res.* 113, C00B01. doi:10.1029/2007JC004703.
- Bishop, J.K.B., Fleisher, M.Q., 1987. Particulate manganese dynamics in Gulf Stream warm-core rings and surrounding waters of the N.W. Atlantic. *Geochim. Cosmochim. Acta* 51, 2807–2825.
- Bishop, J.K.B., Edmond, J., Ketten, D.R., Bacon, M.P., Silker, W.B., 1977. The chemistry, biology, and vertical flux of particulate matter from the upper 400 m of the Equatorial Atlantic Ocean. *Deep-Sea Res.* 1 511–548.
- Bishop, J.K.B., Schupack, D., Sherrell, R.M., Conte, M., 1985. A Multiple Unit Large Volume in-situ Filtration System (MULVFS) for sampling oceanic particulate matter in mesoscale environments. In: Zirino, A. (Ed.), *Mapping Strategies in Chemical Oceanography*. Advanced in Chemistry Series, vol. 209. American Chemical Society, Washington, D.C., pp. 155–175.
- Buesseler, K.O., Trull, T.V., Steinberg, D.K., Silver, M.W., Siegel, D.A., Saitoh, S.-I., Lamborg, C.H., Lam, P.J., Karl, D.M., Jiao, N.Z., Honda, M.C., Elskens, M., Dehairs, F., Brown, S.L., Boyd, P.W., Bishop, J.K.B., Bidigare, R.R., 2008. VERTIGO (VERTical Transport In the Global Ocean): a study of particle sources and flux attenuation in the North Pacific. *Deep-Sea Res., Part 2* 55, 1522–1539.
- Cardinal, D., Dehairs, F., Cattaldo, T., André, L., 2001. Geochemistry of suspended particles in the SubAntarctic and Polar Frontal Zones south of Australia: constraints on export and advection processes. *J. Geophys. Res.* 106 (C12), 31,637–34,656.
- Charette, M.A., Gonnea, M.E., Morris, P.J., Statham, P.J., Fones, G.R., Planquette, H., Salter, I., Naveira Garabato, A., 2007. Radium isotopes as tracers of iron sources fueling a Southern Ocean phytoplankton bloom. *Deep-Sea Res., Part 2* 54, 1989–1998.
- Coale, K.H., Gordon, M., Wang, X., 2005. The distribution and behavior of dissolved and particulate iron and zinc in the Ross Sea and Antarctic circumpolar current along 170°W. *Deep-Sea Res.* 1 52, 295–318.
- Cullen, J.T., Sherrell, T.M., 1999. Techniques for determination of trace metals in small samples of size-fractionated particulate matter: phytoplankton metals off central California. *Mar. Chem.* 67, 233–247.
- De Baar, H.J.W., de Jong, J.T.M., 2001. Distributions, sources and sinks of iron in seawater. In: Turner, D., Hunter, K.A. (Eds.), *The Biogeochemistry of Iron in Seawater*. John Wiley, Hoboken, N.J., pp. 125–253.
- De Baar, H.J.W., de Jong, J.T.M., Bakker, D.C.E., Löscher, B.M., Veth, C., Bathmann, U., Smetacek, V., 1995. Importance of iron for plankton blooms and carbon dioxide drawdown in the Southern Ocean. *Nature* 373, 412–415. doi:10.1038/373412a0.
- Dehairs, F., Goeyens, L., Stroobants, N., Mathot, S., 1992. Elemental composition of suspended matter in the Scotia–Weddell confluence area during spring and summer 1988 (EPOS Leg 2). *Polar Biol.* 12, 25–33.
- Eggiman, D.W., Betzer, P.R., 1976. Decomposition and analysis of refractory oceanic suspended materials. *Anal. Chem.* 48, 886–890.
- Fielding, S., Ward, P., Pollard, R.T., Seeyave, S., Read, J.F., Hughes, J.A., Smith, T., Castellani, C., 2007. Community structure and grazing impact of mesozooplankton during late/early summer 2004/2005 in the vicinity of the Crozet Islands (Southern Ocean). *Deep-Sea Res., Part 2* 54, 2106–2125.
- Fitzwater, S.E., Johnson, K.S., Elrod, V.A., Ryan, J.P., Coletti, L.J., Tanner, S.J., Gordon, R.M., Chavez, F.P., 2003. Iron, nutrient and phytoplankton biomass relationships in upwelled waters of the California coastal system. *Cont. Shelf Res.* 23, 1523–1544.
- Frew, R.D., Hutchins, D.A., Nodder, S., Sanudo-Wilhelmy, S., Tovar-Sanchez, A., Leblanc, K., Hare, C.E., Boyd, P.W., 2006. Particulate iron dynamics during Fe cycle in SubAntarctic waters southeast of New Zealand. *Glob. Biogeochem. Cycles* 20, GB1593. doi:10.1029/2005GB002558.
- Gardner, W.D., 2000. Sediment trap technology and sampling in surface waters. In: Hanson, R.B., Ducklow, H.W., Field, J.G. (Eds.), *The Changing Ocean Carbon Cycle: a Midterm Synthesis of the Joint Global Ocean Flux Study*. Cambridge University Press, pp. 240–281.
- Goldberg, E.D., Arrhenius, G.O.S., 1958. Chemistry of Pacific pelagic sediments. *Geochim. Cosmochim. Acta* 13 (2–3), 153–198.
- Grotti, M., Soggia, F., Abelmoschi, M.L., Rivaro, P., Magi, E., Frache, R., 2001. Temporal distribution of trace metals in Antarctic coastal waters. *Mar. Chem.* 76 (3), 189–209.
- Gunn, B.M., Coyyll, R., Watkins, N.D., Abranson, C.E., Nougier, J., 1970. Geochemistry of an Oceanite–Ankaramite–Basalt Suite from East-Island, Crozet Archipelago. *Contrib. Mineral. Petrol.* 28 (4), 319–329.
- Hedges, J.I., Baldock, J.A., Gelinas, Y., Lee, C., Peterson, M.L., Wakeham, S.G., 2002. The biochemical and elemental compositions of marine plankton: a NMR perspective. *Mar. Chem.* 78, 48–63.
- Jacquet, S.H.M., Dehairs, F., Savoye, N., Obermosterer, I., Christaki, U., Monnin, C., Cardinal, D., 2008. Mesopelagic organic carbon remineralisation in the Kerguelen Plateau region tracked by biogenic particulate Ba. *Deep-Sea Res., Part 2* 55, 868–879.
- Kuss, J., Kremling, K., 1999. Particulate trace element fluxes in the deep northeast Atlantic Ocean. *Deep-Sea Res.* 1 46, 149–169.
- Lam, P.J., Bishop, J.K.B., Henning, C.C., Marcus, M.A., Waychunas, G.A., Fung, I.Y., 2006. Wintertime phytoplankton bloom in the subarctic Pacific supported by continental margin iron. *Glob. Biogeochem. Cycles* 20 (1), GB1006. doi:10.1029/2005GB002557.
- Lampitt, R.S., Boorman, B., Brown, L., Lucas, M.I., Salter, I., Sanders, R., Saw, K., Seeyave, S., Thomalla, S.J., Turnewitsch, R., 2008. Particle export from the euphotic zone: estimates using a novel drifting sediment trap, ²³⁴Th and new production. *Deep-Sea Res.* 1 55 (11), 1484–1502. doi:10.1016/j.dsr.2008.07.002.
- Landing, W.M., Bruland, K.W., 1987. The contrasting biogeochemistry of iron and manganese in the Pacific Ocean. *Geochim. Cosmochim. Acta* 51, 29–43.
- Lewis, B.L., Landing, W.M., 1992. The investigation of dissolved and suspended particulate trace metal fractionation in the Black Sea. *Mar. Chem.* 40, 105–141.
- Löscher, B.M., 1999. Relationships among Ni, Cu, Zn, and major nutrients in the Southern Ocean. *Mar. Chem.* 67, 67–102.
- Löscher, B.M., De Baar, H.J.W., de Jong, J.T.M., Veth, C., Dehairs, F., 1997. The distribution of Fe in the Antarctic Circumpolar Current. *Deep-Sea Res., Part 2* 44 (1–2), 143–187.
- Morel, F.M.M., Price, N.M., 2003. The biogeochemical cycles of trace metals in the oceans. *Science* 300, 944–947.
- Morris, P.J., Sanders, R., Turnewitsch, R., Thomalla, S.J., 2007. ²³⁴Th derived particulate organic carbon export compared to new production from an island induced phytoplankton bloom in the Southern Ocean. *Deep-Sea Res., Part 2* 54, 2208–2232.
- Mortlock, R.A., Froelich, P.N., 1989. A simple method for the rapid-determination of biogenic opal in pelagic marinesediments. *Deep-Sea Res.* A 36 (9), 1415–1426.
- Murray, R., Leinen, M., Isern, A., 1993. Biogenic flux of Al to sediment in the Central Equatorial Pacific Ocean: evidence for increased productivity during glacial periods. *Paleoceanography* 8 (5), 651–670.
- Murray, R., Knowlton, C., Leinen, M., Mix, A., Polsky, C., 2000. Export production and carbonate dissolution in the Central Equatorial Pacific Ocean over the past 1 Myr. *Paleoceanography* 15 (6), 570–592.
- Planquette, H., Statham, P.J., Fones, G.R., Charette, M.A., Moore, C.M.M., Salter, I., Nédélec, F.H., Taylor, S.L., French, M., Baker, A.R., Mahowald, N., Jickells, T.D., 2007. Dissolved iron in the vicinity of the Crozet Islands, Southern Ocean. *Deep-Sea Res., Part 2* 1999–2019.
- Pollard, R.T., Sanders, R., Lucas, M.I., Statham, P.J., 2007a. The Crozet Natural Iron Bloom and Export Experiment (CROZEX). *Deep-Sea Res., Part 2* 54, 1905–1914.
- Pollard, R.T., Venables, H.J., Read, J.F., Allen, J.T., 2007b. Large scale circulation around the Crozet Plateau controls an annual phytoplankton bloom in the Crozet Basin. *Deep-Sea Res., Part 2* 54, 1915–1929.
- Poulton, A.J., Moore, C.M., Seeyave, S., Lucas, M.I., Fielding, S., Ward, P., 2007. Phytoplankton community composition around the Crozet Plateau, with emphasis on diatoms and phaeocystis. *Deep-Sea Res.* 54, 2085–2105.
- Read, J.F., Pollard, R.T., Allen, J.T., 2007. Sub-mesoscale structure and the development of an eddy in the SubAntarctic Front north of the Crozet Islands. *Deep-Sea Res., Part 2* 1930–1948.
- Saito, C., Noriki, S., Tsunogai, S., 1992. Particulate flux of Al, a component of land origin in the western North Pacific. *Deep-Sea Res.* 39, 1315–1327.
- Salter, I., Lampitt, R.S., Sanders, S., Poulton, A.J., Kemp, A.E.S., Boorman, B., Saw, K., Pearce, R., 2007. Estimating carbon, silica and aluminum export from a naturally fertilised phytoplankton bloom in the Southern Ocean using PELAGRA: a novel drifting sediment trap. *Deep-Sea Res.* 54. doi:10.1016/j.dsr.2007.07.008.
- Seeyave, S., Lucas, M.I., Moore, C.M., Poulton, A.J., 2007. Phytoplankton productivity and community structure across the Crozet Plateau during summer 2004/2005. *Deep-Sea Res., Part 2* 54, 2020–2044.
- Sherrell, R.M., Boyle, E.A., 1992. The trace metal composition of suspended particles in the oceanic water column near Bermuda. *Earth Planet. Sci. Lett.* 111, 155–174.
- Strickland, J.D.H., Parsons, T.R., 1968. Inorganic micronutrients in seawater. In: Stevenson, J.C. (Ed.), *A Practical Handbook of Seawater Analysis*. Fisheries Research Board of Canada, Ottawa, pp. 45–137.
- Strzepek, R.F., Maldonado, M.T., Higgins, J.L., Hall, J., Safi, K., Wilhelm, S.W., Boyd, P.W., 2005. Spinning the “ferrous wheel”: the importance of the microbial community in an iron budget during the FeCycle experiment. *Glob. Biogeochem. Cycles* 19, GB4s26. doi:10.1029/2005GB002490.
- Stumm, W., 1992. *Chemistry of the Solid–Water interface*, ed. Wiley, New York.

- Tovar-Sanchez, A., Sañudo-Wilhelmy, S.A., Garcia-Vargas, M., Weaver, R.S., Popels, L.C., Hutchins, D.A., 2003. A trace metal clean reagent to remove surface-bound iron from marine phytoplankton. *Mar. Chem.* 82, 91–99.
- Valdes, J.R., Price, J.F., 2000. A neutrally buoyant, upper ocean sediment trap. *J. Atmos. Ocean. Technol.* 17, 62–68.
- Van Cappellen, P., Qiu, L., 1997a. Biogenic silica dissolution in sediments of the Southern Ocean. II. Kinetics. *Deep-Sea Res., Part 2* 44, 1109–1128.
- Van Cappellen, P., Qiu, L., 1997b. Biogenic silica dissolution in sediments of the Southern Ocean. I. Solubility. *Deep-Sea Res., Part 2* 44, 1129–1149.
- Venables, H.J., Pollard, R.T., Popova, E.E., 2007. Physical conditions controlling the early development of a regular phytoplankton bloom north of the Crozet Plateau, Southern Ocean. *Deep-Sea Res., Part 2* 54, 1949–1965.
- Verado, D.J., Froelich, P.N., McIntyre, A., 1990. Determination of organic carbon and nitrogen in marine sediments using the Carlo-Erba NA-1500 analyser. *Deep-Sea Res. I* 37, 157–165.
- Weinstein, S.E., Moran, S.B., 2004. Distribution of size-fractionated particulate trace metals collected by bottles and in-situ pumps in the Gulf of Maine–Scotian Shelf and Labrador Sea. *Mar. Chem.* 87, 121–135.
- Wells, M.L., Mayer, L.M., Guillard, R.R.L., 1991. A chemical method for estimating the availability of iron to phytoplankton in seawater. *Mar. Chem.* 33, 23–40.
- Wells, M.L., Smith, G.J., Bruland, K.W., 2000. The distribution of colloidal and particulate bioactive metals in Narragansett Bay, RI. *Mar. Chem.* 71, 143–163.
- Wolff, G., 2007. Benthic Crozet Initial Cruise Report, D300. University of Liverpool.